math xmlns="http://www.w3.org/1998/Math/MathML" display="inline">mi>β/mi>/math>-Delayed One and Two Neutron Emission Probabilities Southeast of math xmlns="http://www.w3.org/1998/Math/MathML" display="inline">mrow>mmultiscripts>mrow>mi>Sn/mi>/mrow>mprescripts>/mprescripts>none>/none>mrow>mn>132/mn>/mrow>/mmultiscripts>/mrow>/math> and the Odd-Even Systematics in math xmlns="http://www.w3.org/1998/Math/MathML" display="inline">mi>r/mi>/math>-Process Nuclide Abundances

V. H. Phong et al.

Phys. Rev. Lett. **129**, 172701 — Published 18 October 2022

DOI: 10.1103/PhysRevLett.129.172701

β-Delayed One and Two Neutron Emission Probabilities South-East of ^{132}Sn and the Odd-Even Systematics in r-process Nuclide Abundances

V. H. Phong,[1,2,*] S. Nishimura,[1,†] G. Lorusso,[1,3,4] T. Davinson,[5] A. Estrade,[6] O. Hall,[5] T. Kawano,[7] J. Liu,[1,8] F. Montes,[9] N. Nishimura,[10,1] R. Grzywacz,[11] K.P. Rykaczewski,[12] J. Agramunt,[13] D.S. Ahn,[1,14] A. Algora,[13] J.M. Allmond,[12] H. Baba,[1] S. Bae,[14] N.T. Brewer,[12,11] C.G. Bruno,[5] R. Caballero-Folch,[15] F. Calviño,[16] P.J. Coleman-Smith,[17] G. Cortes,[16] I. Dillmann,[15,18] C. Domingo-Pardo,[13] A. Fijalkowska,[19] N. Fukuda,[1] S. Go,[1] C.J. Griffin,[5] J. Ha,[1,20] L.J. Harkness-Brennan,[21] T. Isobe,[1] D. Kahl,[5,22] L.H. Khiem,[23,24] G.G. Kiss,[1,25] A. Korgul,[19] S. Kubono,[1] M. Labiche,[17] I. Lazarus,[17] J. Liang,[26] Z. Liu,[27,28] K. Matsui,[1,29] K. Miernik,[19] B. Moon,[14] A.I. Morales,[13] P. Morrall,[17] N. Nepal,[6] R.D. Page,[21] M. Piersa-Siłkowska,[19] V.F.E. Pucknell,[17] B. C. Rasco,[12] B. Rubio,[13] H. Sakurai,[1,29] Y. Shimizu,[1] D.W. Stracener,[12] T. Sumikama,[1] H. Suzuki,[1] J.L. Tain,[13] H. Takeda,[1] A. Tarifeño-Saldivia,[16,13] A. Tolosa-Delgado,[13] M. Wolińska-Cichocka,[30] P.J. Woods,[5] and R. Yokoyama[11,31]

[1] *RIKEN Nishina Center, Wako, Saitama, 351-0198, Japan*
[2] *University of Science, Vietnam National University, Hanoi, 120062, Vietnam*
[3] *National Physical Laboratory, Teddington, TW11 0LW, UK*
[4] *Department of Physics, University of Surrey, Guildford, GU2 7XH, UK*
[5] *School of Physics and Astronomy, University of Edinburgh, Edinburgh, EH9 3FD, UK*
[6] *Department of Physics, Central Michigan University, Mount Pleasant, MI, 48859, USA*
[7] *Theoretical Division, Los Alamos National Laboratory, Los Alamos, NM 87545, USA*
[8] *Department of Physics, University of Hong Kong, Pokfulman Road, Hong Kong*
[9] *National Superconducting Cyclotron Laboratory, East Lansing, MI, 48824, USA*
[10] *Astrophysical Big-Bang Laboratory, Cluster for Pioneering Research, RIKEN, Wako, Saitama, 351-0198, Japan*
[11] *University of Tennessee, Knoxville, TN, USA*
[12] *Physics Division, Oak Ridge National Laboratory, Oak Ridge, TN 37831, USA*
[13] *Instituto de Fsica Corpuscular, CSIC and Universitat de Valencia, E-46980 Paterna, Spain*
[14] *Center for Exotic Nuclear Studies, Institute for Basic Science, Daejeon 34126, Republic of Korea*
[15] *TRIUMF, Vancouver BC, V6T 2A3, Canada*
[16] *Universitat Politecnica de Catalunya, E-08028 Barcelona, Spain*
[17] *STFC Daresbury Laboratory, Daresbury, Warrington, WA4 4AD, UK*
[18] *Department of Physics and Astronomy, University of Victoria, Victoria BC, V8P 5C2, Canada*
[19] *Faculty of Physics, University of Warsaw, PL02-093 Warsaw, Poland*
[20] *Seoul National University, Department of Physics and Astronomy, Seoul 08826, Republic of Korea*
[21] *Department of Physics, University of Liverpool, Liverpool, L69 7ZE, UK*
[22] *Extreme Light Infrastructure – Nuclear Physics, Horia Hulubei National Institute for R&D in Physics and Nuclear Engineering (IFIN-HH), 077125 Bucharest-Măgurele, Romania*
[23] *Institute of Physics, Vietnam Academy of Science and Technology, Ba Dinh, 118011 Hanoi, Vietnam*
[24] *Graduate University of Science and Technology, Vietnam Academy of Science and Technology, Cau Giay, 122102 Hanoi, Vietnam*
[25] *Institute for Nuclear Research (Atomki), Debrecen, H4032, Hungary*
[26] *McMaster University, Department of Physics and Astronomy, Hamilton ON, L8S 4M1, Canada*
[27] *Institute of Modern Physics, Chinese Academy of Sciences, Lanzhou 730000, China*
[28] *School of Nuclear Science and Technology, University of Chinese Academy of Sciences, Beijing 100049, China*
[29] *University of Tokyo, Department of Physics, Tokyo 113-0033, Japan*
[30] *Heavy Ion Laboratory, University of Warsaw, Pasteura 5A, PL-02-093 Warsaw, Poland*
[31] *Center for Nuclear Study, University of Tokyo, RIKEN Campus, 2-1 Hirosawa, Wako, Saitama 351-0198, Japan*

(Dated: August 24, 2022)

The β-delayed one and two neutron emission probabilities (P_{1n} and P_{2n}) of 20 neutron-rich nuclei with $N \geq 82$ have been measured at the RIBF facility of the RIKEN Nishina Center. P_{1n} of ^{130,131}Ag, ^{133,134}Cd, ^{135,136}In and ^{138,139}Sn were determined for the first time and stringent upper limits were placed on P_{2n} for nearly all cases. β-delayed two-neutron emission ($\beta 2n$) was unambiguously identified in ^{133}Cd, ^{135,136}In and their P_{2n} were measured. Weak $\beta 2n$ was also detected from ^{137,138}Sn. Our results highlight the effect of the $N = 82$ and $Z = 50$ shell closures on β-delayed neutron emission probability and provides stringent benchmarks for newly developed macroscopic-microscopic and self-consistent global models with the inclusion of a statistical treatment of neutron and γ-emission. The impact of our measurements on r-process nucleosynthesis was studied in a neutron star merger scenario. Our P_{1n} and P_{2n} have a direct impact on the odd-even staggering of

the final abundance, improving the agreement between calculated and observed solar system abundances. The odd isotope fraction of Ba in r-process enhanced (r-II) stars is also better reproduced using our new data.

The nucleosynthesis of elements heavier than iron via the rapid neutron-capture (r-) process has been the subject of intense studies since its mechanism was first proposed [1, 2]. In recent decades, remarkable progress has been made on many fronts, including the advancement of astrophysical simulations, the detection of multi-messenger events associated with gravitational waves, and observations of metal-poor stars in the Milky Way halo and in ultra-faint dwarf galaxies [3–5]. In these contexts, the second r-process abundance peak (with the mass number $A \sim 130$) plays a crucial role. Recent observations of Te in metal-poor stars by the Hubble Space Telescope [6–8] have shown that the peak is produced along with the rare-earth elements, but with a larger variability across stars that is not yet fully understood [9, 10]. This is possibly linked to the sensitivity of the peak to the r-process conditions or to contributions from other nucleosynthesis processes [11, 12]. Observation of Te and Cs have been tentatively reported in the near-infrared during the kilonova event following neutron star merger GW170817 [13]. Conclusive data is likely to require future 30 m class telescopes [14] that may provide invaluable new information on the second r-process peak. Detection of other elements such as Sb, I, and Xe, may also be possible [13]. In addition, the next generation of space observatories [15, 16] may be able to detect γ-rays from the radioactive decay of the peak's progenitors [17].

To connect the growing body of observations to astrophysics models and ultimately derive the r-process conditions, knowledge of the properties of the second r-process peak radioactive progenitors is essential. The peak has long been associated with the reduced neutron capture cross-sections of nuclei with neutron number $N = 82$, which would cause such isotones to build up. The r-process matter flow would then break out of the $N = 82$ shell below atomic number $Z = 50$. Here, the nucleosynthesis path involves unstable nuclei which decay by β-delayed neutron emission (βn) – a process where due to the large β-decay Q values, neutron-unbound states are populated in the daughter nuclei. Following the exhaustion of free neutrons, the r-process freezes out and the second peak originates from a complex network of competing reactions including βn, neutron captures, and photodisintegration reactions. Depending on the neutron richness of the astrophysical environment, fission of heavy nuclei near the endpoint of the r-process ($A > 260$) will also contribute to the second peak [18–20].

In this Letter, we report measurements of β-decay halflives and β-delayed one- and two-neutron emission probabilities (P_{1n} and P_{2n}) south-east of ^{132}Sn, reaching the edge of r-process paths predicted by several r-process models [21, 22]. P_{xn} in this region are key to model accurately the $A \sim 130$ peak. Theoretical P_{xn} value predictions show large discrepancies [23, 24] and their reliability is limited by the strong sensitivity to experimentally unknown nuclear structure details such as masses, neutron separation energies, β-decay strength distributions and densities of states. In addition, near the r-process path, β-delayed multi-neutron emission channels are expected, with competition between different channels posing an additional modelling challenge. Relevant to the r-process nucleosynthesis ($Z > 28$), only six strong $\beta 2n$ emitters ($P_{2n} > 1\%$) have been measured to date [25–28], and only one of them (^{134}In) lays south-east of ^{132}Sn [27]. Our data provide new experimental inputs for r-process calculations and a new testing ground for models required to predict P_{xn} of r-process nuclei unreachable today.

Neutron-rich nuclei were produced by in-flight fission of a ∼50 pnA, 345 MeV/nucleon ^{238}U beam impinging on a 4 mm Be target. Fission fragments were separated using the BigRIPS separator [29] and identified on an event-by-event basis using energy loss, time-of-flight and magnetic rigidity information [30] before being implanted into the stack of six highly segmented silicon detectors of the Advanced Implantation Detector Array (AIDA)[31]. Fig. 1 shows a particle identification plot of the implanted ions.

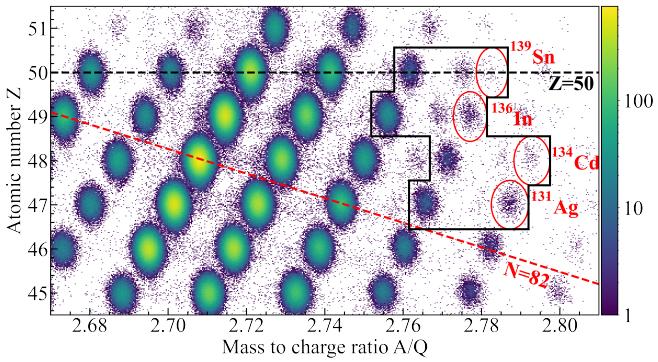

FIG. 1. Particle identification plot of ions implanted in AIDA. The black contour highlights the isotopes with P_n measured for the first time in this work. The heaviest isotope reported in this work is labeled for each element.

AIDA was surrounded by two clover-type HPGe detectors [40] and the BRIKEN neutron detector consisting of 140 ^{3}He proportional counters embedded in a high-density polyethylene moderator [41, 42]. The neutron detection efficiency was carefully modeled using GEANT4 Monte-Carlo simulations [42] and validated by measurements of a ^{252}Cf neutron source [43]. It is nearly constant

TABLE I. β-decay half-lives, P_{1n} and P_{2n} measured in this work and reported in the literature. Literature half-lives are from Lorusso et al. [32] unless stated otherwise. The nuclei with a possible mixture of β-decays from ground and milliseconds isomeric states are tagged with an asterisk (*).

Nuclide	$T_{1/2}^{exp.}$ [ms]	$T_{1/2}^{lit.}$ [ms]	P_{1n} [%]	P_{2n} [%]	P_{1n} lit. [%]	Nuclide	$T_{1/2}^{exp.}$ [ms]	$T_{1/2}^{lit.}$ [ms]	P_{1n} [%]	P_{2n} [%]	P_{1n} lit. [%]
^{129}Ag*	53.6(13)	52(4)	$18.6^{+1.7}_{-0.9}$	<1.2	17.9(14) [23]	^{133}In*	166(4)	163(7)	89(5)	<1.2	90(3)% [33][a]
^{130}Ag	44(3)	42(5)	66(6)	<5	-	^{134}In[b]	127(2)	126(7)	86^{+2}_{-4}	$11.9^{+1.2}_{-0.8}$	89(3) [27]
^{131}Ag	35(5)	35(8)	100^{+0}_{-6}	<6	-	^{135}In	104(4)	103(5)	88^{+2}_{-5}	9.3(1.3)	-
^{130}Cd	135(2)	127(2)	2.9(2)	0	3.0(2) [23]	^{136}In	90(10)	85^{+10}_{-8}	84(10)	12.8(5)	-
^{131}Cd	100(2)	68(3) [34]	$13.5^{+1.1}_{-0.7}$	<0.7	3.5(1) [34]	^{134}Sn	1019(34)	890(20)	24.1(15)	0	17(13) [35]
		98.0(2)				^{135}Sn	514(30)	515(5)	20(2)	<2.5	21(3) [36]
^{132}Cd	82.5(9)	97(10) [34]	100^{+0}_{-6}	<1.7	60(15) [34]	^{136}Sn	366(5)	300(15) [37]	$18.5^{+2.4}_{-1.3}$	<0.37	27(4) [37]
		82(4)						350(5)			
^{133}Cd	61(6)	64(8)	86(7)	6(2)	-	^{137}Sn	231(7)	273(7) [37]	23(2)	0.45(24)	50(10) [37]
^{134}Cd	38(31)	65(15)	65(26)	<39	-			230(30)			
^{131}In*	278(7)	261(3)	2.9(3)	0	2.3(3) [38][c]	^{138}Sn	150(21)	140^{+30}_{-20}	28(5)	1.8(13)	-
^{132}In	214(8)	198(2)	12.2(12)	<1.6	12.3(4) [39]	^{139}Sn	139(61)	130(60)	56(34)	<86	-

[a] For the $9/2^+$ ground state. P_{1n} = 93(3)% for $21/2^+$ isomeric state [33].
[b] P_{2n} = 9(2)% [27].
[c] For the combined $9/2^+$ ground state and $1/2^-$ isomeric state. P_{1n} = 12(7)% for the $21/2^+$ isomeric state [38].

up to 1 MeV with an average value of 66.8(20)%, dropping to about 59% at 3 MeV [41, 44]. The systematic uncertainty introduced by the unknown neutron spectra was estimated as in Ref. [45]. Signals from all our detectors were recorded by digital acquisition systems synchronized with BigRIPS [31, 46].

Implanted ions were correlated with electrons from subsequent β decays on the basis of detection time and position in the silicon detectors [47]. Neutrons were correlated with β-decays within a 400 μs time window, needed to account for the neutron thermalization. The unbinned distribution of time differences between implantations and correlated β-decays with their associated neutron multiplicity were fitted using the maximum likelihood method to determine simultaneously half-lives and P_{xn} values. The fits employ probability density functions that include a parent, all daughter's activities, neutron background, and consider the β and neutron efficiency of the detector setup [41, 48, 49].

The P_{1n} and P_{2n} measured in this work are reported in Tab. I. They are in good agreement with the literature values for In isotopes, but large differences were found for ^{131,132}Cd and ^{136,137}Sn [34, 37], also in the half-lives. Half-lives from this work are generally consistent with the previous measurements performed at RIBF [32, 47], although differences for ^{130}Cd, ^{131,132}In and ^{134,136}Sn of $\lesssim$10% are not fully understood. The reason of these differences can be related to the employed β-counting systems.

P_{xn} systematics are shown in Fig. 2, where an abrupt increase of the P_{1n} at $N = 84$ is observed for Cd, In and Sn isotopes. Such an increase of P_{1n} clearly correlates with the sudden drop of neutron separation energy S_n in daughter nuclei beyond the $N = 82$ shell gap. The relatively small P_{1n} of Sn isotopes reflects the small Q_β of these isotopes relative to their lighter isotones. This is due to the $Z = 50$ proton shell closure. For Ag isotopes, a large P_{1n} value increase occurs at $N = 83$ (^{130}Ag) rather than $N = 84$. This behaviour departs from the systematic trend highlighted above, and is somewhat unexpected considering that S_n in the daughter nucleus ^{130}Cd is rather large (6.06(2) MeV [50]). Further investigation, e.g., via neutron spectroscopy, is needed to explain this behaviour.

Our P_{1n} and P_{2n} were compared with the predictions of two theoretical models, the quasiparticle random-phase approximation (QRPA) [52, 53] based on the microscopic-macroscopic Finite Range Droplet Model (FRDM) [54] and the Relativistic Hartree-Bogoliubov (RHB) plus proton-neutron QRPA (pnQRPA) [55]. The latest versions of these models incorporate the treatment of the β-delayed emission phase under the framework of the Hauser-Feshbach (HF) statistical model with nominal level densities [56–59]. We find that for the In isotopes, the inclusion of HF vastly improves model predictions that would otherwise grossly overestimate the P_{2n}/P_{1n} ratios. However, for FRDM+QRPA+HF this is true only up to ^{135}In; the large drop for theoretical P_{1n} in ^{136}In is not observed experimentally. The reason for this is unclear, the attempt to tune the level density of ^{135}Sn was not sufficient as it showed that a modification of few orders of magnitude would be required to match our data. The inclusion of the HF model improves to some extent the predictions for Cd isotopes, but the cal-

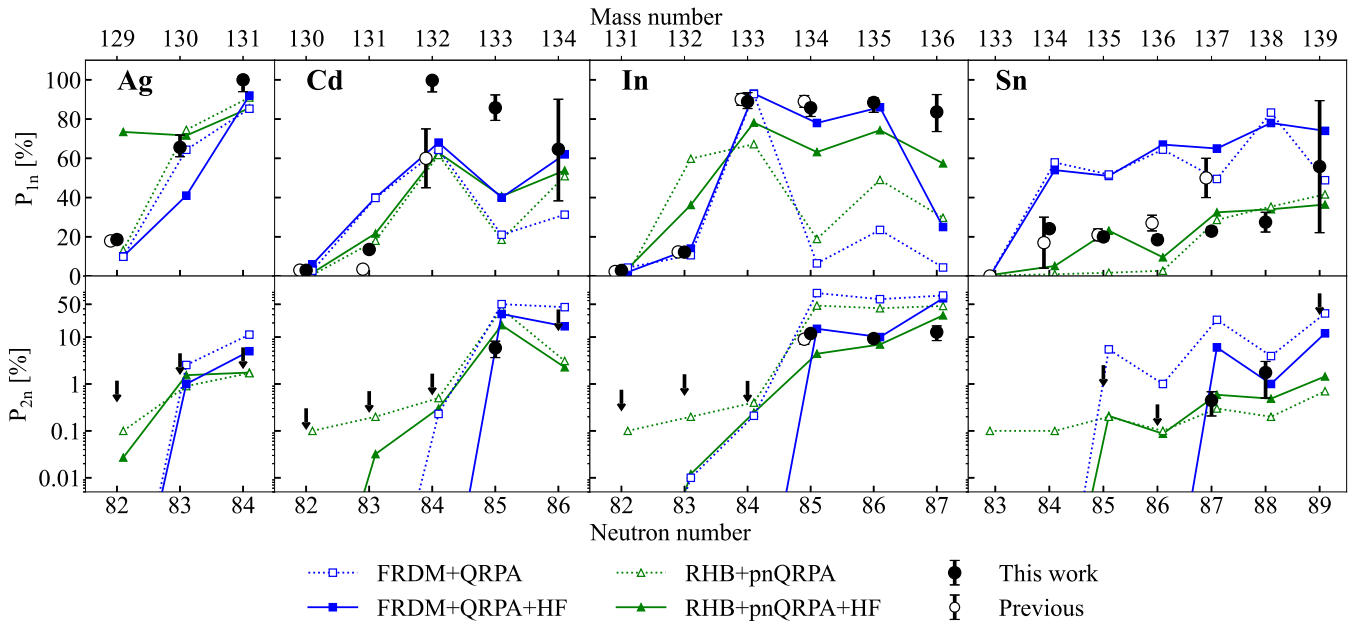

FIG. 2. Systematics of measured P_{1n} (middle panels) and P_{2n} compared with literature values [23, 27, 33–39, 51] and theoretical calculations.

culations still fail to reproduce the experimental values, while in Ag isotopes the inclusion of HF worsen the predictions. In the case of the Sn isotopes, FRDM+QRPA systematically overestimates P_{1n} by nearly a factor of three. RHB+pnQRPA+HF performs better, however, it systematically underestimates half-lives by about a factor of 5, and underestimates P_n values for $N < 82$. Therefore, in the following r-process calculations we use both models.

To understand the role of the measured P_{xn} and their impact in the astrophysical r-process, we have carried out reaction network calculations using the SkyNet [60] and Nucnet [61] codes with reaction rates from the JINA REACLIB V2.2 database [62]. β-decay rates were updated with the P_{xn} values from this work, neutron-induced and spontaneous fission was considered as in Ref. [63]. We chose r-process conditions typical of merging neutron stars [64] with entropy $S^b = 12\ k_B$/baryon, electron fraction $Y_e^b = 0.062$, and expansion timescale $\tau^b = 66$ ms. These conditions (baseline calculation) were found to best reproduce the solar system abundance in the mass range $A = 129 - 139$, which is the one most effected by our P_n values.

The nuclear reaction flow during freezeout for the baseline calculation is shown in Fig. 3(a). One notices that the progenitors for the elements of the second peak are all βn emitters (produced either by neutron capture or fission). Many of such progenitors are included in our measurements and some of their P_{xn} values are critical to determine the pathway to stability of neutron-rich material. For example, the abundance of ^{130}Te is produced predominantly by a βn flow from ^{131}Ag, the P_n value of ^{129}Ag affects the flow to ^{128}Te, ^{132}Xe receives a large contribution from the βn of ^{134}Cd and ^{133}In. ^{133}Cs is critically affected by the βn flows from ^{134}In, ^{135}In and ^{134}Cd. The P_{xn} values for these isotopes are now experimentally known. Among the isotopes affected by our data, ^{128,130}Te, ^{133}Cs and ^{136}Xe are particularly important because they are exclusively produced in the r-process, so their abundance uncertainty is small.

To quantify the impact of our experimental P_{xn} values on the final abundances, we compared the abundances produced by our baseline simulation to those of three other calculations where the P_{xn} values of interest are set to the values predicted by the FRDM+QRPA+HF, RHB+pnQRPA+HF, and EDM models. EDM is a phenomenological multiple-neutron emission model based on a level density function with parameters empirically determined from existing experimental data [66]. The resulting final abundances and their corresponding changes relative to the baseline calculation are shown in Figs. 3(b,c). Differences of up to 30% are found when using the theoretical P_n values. The shadowed area provides an estimate of the r-process calculations uncertainty removed by our measurement. Notably, when FRDM+QRPA+HF values are used, the odd-even staggering beyond mass $A = 132$ is less pronounced. This is mainly due to the model overestimation of P_{1n} values for Sn isotopes (see Fig. 2). The calculations above were repeated over the large parameter space $Y_e = 0.005 - 0.062$ suitable to produce nuclei in the mass range $A = 129 - 139$. In this Y_e range the r-process abundance

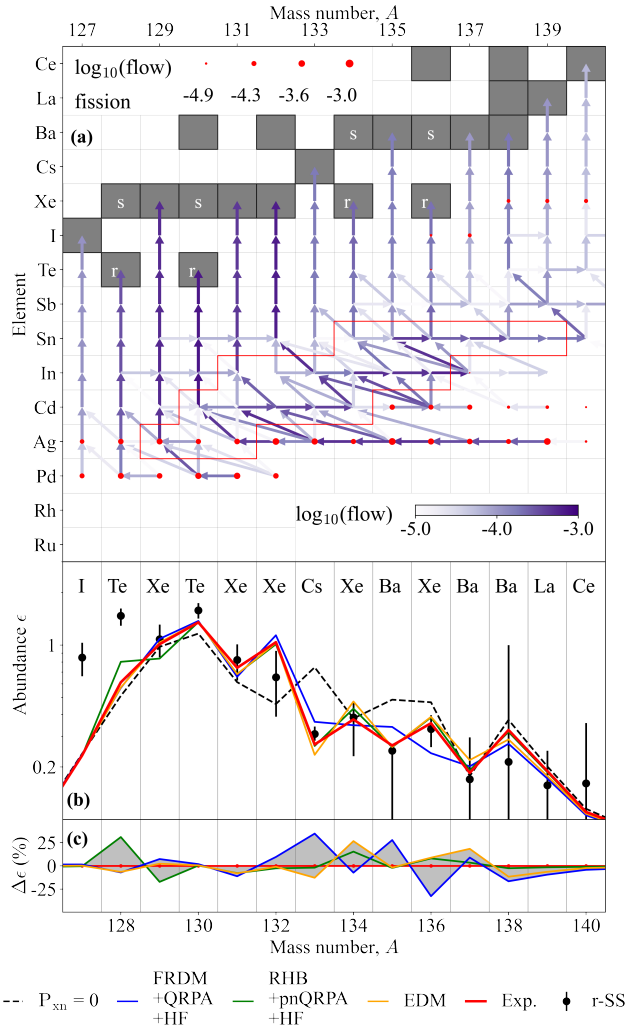

FIG. 3. (a) Time-integrated reaction flows during r-process freeze out. The flows from fission reactions are marked with solid red circles with size proportional to their strength. The flows of other reactions and β-decays are indicated by arrows weighted by their strength. The enclosed red line indicates the nuclear region of interest in this work. Stable isotopes are indicated as gray-filled squares, with those produced only by the slow neutron-capture process and the r-process are tagged as "s" and "r", respectively. (b) Calculated r-process abundances using P_{1n} and P_{2n} from this work and from theoretical models (solid lines). A calculation with $P_{xn} = 0$ (black dash) is reported to identify the abundances most affected by βn. Solar abundances [65] are shown as black circles. (c) Abundance changes $\Delta\epsilon$ (in %) for different models relative to the baseline calculation, and combined as gray bands.

pattern is formed robustly and the odd-even pattern does not change, hence we consider our conclusion on the role of our measurements robust.

The impact of the new measurements on the odd-even abundance pattern can also be tested against Ba observations in r-process enhanced metal-poor stars. Differences in the hyperfine structure splitting among Ba isotopes allow the determination of odd-mass Ba isotope abundances relative to the total Ba abundance ($f_{odd,Ba}$) [67]. $f_{odd,Ba}$ is an important indicator of isotopic composition, useful in characterizing the relative contribution of r- and s-process abundances. Fig. 4 shows the $f_{odd,Ba}$ measured in five r-II stars with strongly enhanced r-process [68] along with the value calculated using experimental P_{xn} (red band). The figure also shows the range of $f_{odd,Ba}$ calculated using P_{xn} predicted by the three models considered in this paper (shaded band). The comparison illustrates that the use of experimental P_{xn} leads to a more accurate odd-even abundance reducing the uncertainty in r-process calculations. Note that $f_{odd,Ba}$ in solar system has a large uncertainty due to s-process contaminants, especially in ^{138}Ba. The Ba abundance in metal poor stars is, therefore, an important complementary test of the odd-even pattern in this mass range.

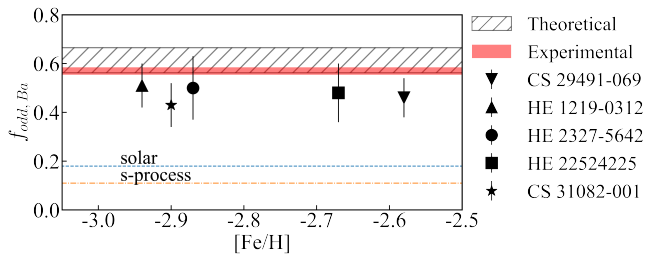

FIG. 4. Odd-mass Ba isotopic fraction $f_{odd,Ba}$ for five r-process enhanced stars (r-II) labeled with their names [68, 69] compared to $f_{odd,Ba}$ calculated using experimental P_{xn} (red band) and a range of $f_{odd,Ba}$ calculated using P_{xn} predicted by the three models considered in this paper (shaded area), with FRDM+QRPA+HF resulting in the upper limit and RHB+pnQRPA+HF in the lower one. $f_{odd,Ba}$ for solar (dashed line) and pure s-process (dash-dotted line) abundances [70]. The metallicity $[Fe/H]$ is defined as the logarithm of the iron-to-hydrogen number density ratio normalized to that of the sun.

In summary, we have carried out the measurement of 20 β-delayed neutron emission probabilities for isotopes of Ag, Cd, In, and Sn beyond the $N = 82$ shell closure, reporting 8 new P_{1n}, 5 new P_{2n}, and P_{2n} upper limits for all 20 of the nuclei studied. The new measurements provide a new picture of P_n systematics crossing the $N = 82$ and $Z = 50$ shells that includes for the first time Ag, and extends significantly our knowledge of Cd, In, and Sn. Our P_n for ^{131,132}Cd and ^{136,137}Sn are at variance with previous data. The new measurements provide a new experimental ground to test nuclear models, with P_{2n} being particularly important to test the Hauser-Feshbach model of competition between β-delayed emission channels. Disagreements with theoretical models highlight the importance of experimental measurements. The new data have a direct impact on r-process calculations removing up to nearly 30% of uncertainty deriving from theoretical models, and improving the agreement with

both the solar system and metal poor r-process enhanced star abundances. This is an important new step forward toward a more reliable description of the second abundance peak and of key elements such as Te, Cs, and Ba. Isotopes with two neutrons beyond the limit of this experiment are the next milestone for the study of P_{xn} in this region, likely to complete the set of P_{xn} needed to model the second r-process peak. The observation of isotopes with β_{3n} emission is also of great interest.

This experiment was performed at the RI Beam Factory operated by RIKEN Nishina Center and CNS, University of Tokyo, supported by JSPS KAKENHI (Grants No.: 14F04808, 17H06090, 19H00693, 20H05648, 21H01087, 25247045, 19340074), RIKEN program for Evolution of Matter in the Universe (r-EMU), National Science Foundation under Grants No. PHY-1430152 (JINA Center for the Evolution of the Elements), No. PHY-1565546 (NSCL), and No. PHY-1714153 (Central Michigan University), the Spanish Ministerio de Economa y Competitividad under Grants nos. FPA2014-52823-C2-1-P, FPA2014-52823-C2-2-P, FPA2017-83946-C2-1-P, FPA2017-83946-C2-2-P, Grants from Ministerio de Ciencia e Innovacion No. PID2019-104714GB-C21 and PID2019-104714GB-C22, European Regional Development Fund, Generalitat Valenciana PROMETEO/2019/007, Office of Nuclear Physics, U.S. Department of Energy Award No. DE-FG02-96ER40983 (UTK) and DE- AC05-00OR22725 (ORNL), National Nuclear Security Administration under the Stewardship Science Academic Alliances program through DOE Award No. DE- NA0002132, UK Science and Technology Facilities Council Grant No. ST/N00244X/1, ST/P004598/1 and ST/V001027/1, National Nuclear Security Administration of the U.S. Department of Energy at Los Alamos National Laboratory under Contract No. 89233218CNA000001. B.M, Basic Science in Republic of Korea (Grant No. IBS-R031-Y1), Polish National Science Center under Grants No. 2020/36/T/ST2/00547 and 2019/33/N/ST2/03023, NKFIH (NN128072), JSPS Invitational Fellowships for Research in Japan (ID: L1955) and RIKEN intensive Research Program, and the long-term International Program Associate. SB acknowledges a support from the Institute for Basic Science of the Republic of Korea (Grant No. IBS-R031-D1). Finally, we thank Dr. Zhengyu Xu for the useful discussions.

* phong@ribf.riken.jp
† nishimu@ribf.riken.jp

[1] F. Hoyle, W. A. Fowler, G. R. Burbidge, and E. M. Burbidge, Science **124**, 611 (1956).
[2] E. M. Burbidge, G. R. Burbidge, W. A. Fowler, and F. Hoyle, Rev. Mod. Phys. **29**, 547 (1957).
[3] C. Sneden, J. J. Cowan, and R. Gallino, Annu. Rev. Astron. Astrophys. **46**, 241 (2008).
[4] J. J. Cowan *et al.*, Rev. Mod. Phys. **93**, 015002 (2021).
[5] T. Kajino *et al.*, Prog. Part. Nucl. Phys. **107**, 109 (2019).
[6] I. U. Roederer and J. E. Lawler, Astrophys. J. **750**, 76 (2012).
[7] I. U. Roederer *et al.*, Astrophys. J. **747**, L8 (2012).
[8] I. U. Roederer *et al.*, Astrophys. J. Suppl. Ser. **203**, 27 (2012).
[9] I. U. Roederer *et al.*, Astrophys. J. Suppl. Ser. **260**, 27 (2022).
[10] I. U. Roederer *et al.*, Astrophys. J (to be published).
[11] Y.-Z. Qian and G. Wasserburg, Physics Reports **333-334**, 77 (2000).
[12] F. Montes *et al.*, Astrophys. J **671**, 1685 (2007).
[13] S. J. Smartt *et al.*, Nature **551**, 75 (2017).
[14] TMT project, `https://www.tmt.org`.
[15] V. Tatischeff *et al.*, in *Space Telescopes and Instrumentation 2016: Ultraviolet to Gamma Ray*, Vol. 9905, International Society for Optics and Photonics (SPIE, 2016) pp. 843 – 853.
[16] R. Rando, J. Instrum. **12**, C11024 (2017).
[17] M.-H. Chen, L.-X. Li, D.-B. Lin, and E.-W. Liang, Astrophys. J **919**, 59 (2021).
[18] M. Eichler *et al.*, Astrophys. J. **808**, 30 (2015).
[19] J.-F. Lemaître, S. Goriely, A. Bauswein, and H.-T. Janka, Phys. Rev. C **103**, 025806 (2021).
[20] T. M. Sprouse, M. R. Mumpower, and R. Surman, Phys. Rev. C **104**, 015803 (2021).
[21] S. Shibagaki *et al.*, Astrophys. J. **816**, 79 (2016).
[22] M. R. Mumpower, R. Surman, G. McLaughlin, and A. Aprahamian, Prog. Part. Nucl. Phys. **86**, 86 (2016).
[23] O. Hall *et al.*, Phys. Lett. B **816**, 136266 (2021).
[24] P. Dimitriou *et al.*, Nucl. Data Sheets **173**, 144 (2021).
[25] K. Miernik *et al.*, Phys. Rev. Lett. **111**, 132502 (2013).
[26] R. Yokoyama *et al.*, Phys. Rev. C **100**, 031302(R) (2019).
[27] M. Piersa-Siłkowska *et al.* (IDS Collaboration), Phys. Rev. C **104**, 044328 (2021).
[28] B. Moon *et al.*, Phys. Rev. C **95**, 044322 (2017).
[29] T. Kubo *et al.*, Prog. Theor. Exp. Phys. **2012** (2012), 03C003.
[30] N. Fukuda *et al.*, Nucl. Instrum. Methods Phys. Res., Sect. B **317**, 323 (2013).
[31] C. J. Griffin *et al.*, in *Proceedings of the 14th International Symposium on Nuclei in the Cosmos (NIC2016), JPS Conf. Proc.*, Vol. 14 (2017) p. 020622.
[32] G. Lorusso *et al.*, Phys. Rev. Lett. **114**, 192501 (2015).
[33] J. Benito *et al.* (IDS Collaboration), Phys. Rev. C **102**, 014328 (2020).
[34] M. Hannawald *et al.* (ISOLDE Collaboration), Phys. Rev. C **62**, 054301 (2000).
[35] M. Asghar *et al.*, Nucl. Phys. A **247**, 359 (1975).
[36] J. Shergur *et al.*, Phys. Rev. C **65**, 034313 (2002).
[37] O. Arndt *et al.*, Phys. Rev. C **84**, 061307(R) (2011).
[38] R. Dunlop *et al.*, Phys. Rev. C **99**, 045805 (2019).
[39] K. Whitmore *et al.*, Phys. Rev. C **102**, 024327 (2020).
[40] V. H. Phong *et al.*, Phys. Rev. C **100**, 011302 (2019).
[41] A. Tolosa-Delgado *et al.*, Nucl. Instrum. Methods Phys. Res., Sect. A **925**, 133 (2019).
[42] A. Tarifeño-Saldivia *et al.*, J. Instrum. **12**, 04006 (2017).
[43] M. Pallas *et al.*, arXiv e-prints , arXiv:2204.13379 (2022).
[44] M. Pallas, A. Tarifeno-Saldivia, *et al.*, in preparation.
[45] A. Tolosa-Delgado, *Study of beta-delayed neutron emitters in the region of* ^{78}Ni *and its impact on r-process nucleosynthesis*, Ph.D. thesis (2020), https://roderic.uv.es/handle/10550/76149.

[46] J. Agramunt *et al.*, Nucl. Instrum. Methods Phys. Res., Sect. A **807**, 69 (2016).
[47] O. Hall *et al.*, RIKEN Accel. Prog. Rep. **52**, 38 (2019).
[48] V. H. Phong, S. Nishimura, and L. H. Khiem, Commun. in Physics **28**, 311 (2018).
[49] B. Rasco *et al.*, Nucl. Instrum. Methods Phys. Res., Sect. A **911**, 79 (2018).
[50] M. Wang, W. J. Huang, F. G. Kondev, G. Audi, and S. Naimi, Chin. Phys. C **45**, 030003 (2021).
[51] G. Rudstam, K. Aleklett, and L. Sihver, At. Data Nucl. Data Tables **53**, 1 (1993).
[52] P. Möller, B. Pfeiffer, and K.-L. Kratz, Phys. Rev. C **67**, 055802 (2003).
[53] P. Möller, M. R. Mumpower, T. Kawano, and W. D. Myers, At. Data Nucl. Data Tables **125**, 1 (2019).
[54] P. Möller, A. J. Sierk, T. Ichikawa, and H. Sagawa, At. Data Nucl. Data Tables **109-110**, 1 (2016).
[55] T. Marketin, L. Huther, and G. Martínez-Pinedo, Phys. Rev. C **93**, 025805 (2016).
[56] T. Kawano, P. Möller, and W. B. Wilson, Phys. Rev. C **78**, 054601 (2008).
[57] T. Kawano, P. Talou, M. B. Chadwick, and T. Watanabe, J. Nucl. Sci. Technol. **47**, 462 (2010).
[58] M. R. Mumpower, T. Kawano, and P. Möller, Phys. Rev. C **94**, 064317 (2016).
[59] F. Minato, T. Marketin, and N. Paar, Phys. Rev. C **104**, 044321 (2021).
[60] J. Lippuner and L. F. Roberts, Astrophys. J. Suppl. Ser. **233**, 18 (2017).
[61] B. S. Meyer and D. C. Adams, Meteoritics and Planetary Science Supplement **42**, 5215 (2007).
[62] R. H. Cyburt *et al.*, Astrophys. J. Suppl. Ser. **189**, 240 (2010).
[63] J. Lippuner and L. F. Roberts, Astrophys. J. **815**, 82 (2015).
[64] S. Fujibayashi, S. Wanajo, K. Kiuchi, K. Kyutoku, Y. Sekiguchi, and M. Shibata, Astrophys. J **901**, 122 (2020).
[65] S. Goriely, Astron. Astrophys. **342**, 881 (1999).
[66] K. Miernik, Phys. Rev. C **90**, 054306 (2014).
[67] P. Magain and G. Zhao, Astron. Astrophys. **268**, L27 (1993).
[68] C. Wenyuan, J. Xiaohua, S. Jianrong, Z. Gang, and Z. Bo, Astrophys. J. **854**, 131 (2018).
[69] X. Y. Meng *et al.*, Astron. Astrophys. **593**, A62 (2016).
[70] C. Arlandini *et al.*, Astrophys. J **525**, 886 (1999).